Probing the generalized magicity of Ag nanoclusters constructed on Si(111) by atomic manipulation

Fangfei Ming,[1] Guohua Zhong,[2] Qin Liu,[1] Kedong Wang,[1] Zhenyu Zhang,[3,*] and Xudong Xiao[1,2,*]

[1]*Department of Physics, The Chinese University of Hong Kong, Shatin, New Territory, Hong Kong, China*

[2]*Shenzhen Institute of Advanced Technology, Chinese Academy of Science, Shenzhen, China*

[3]*International Center for Quantum Design of Functional Materials (ICQD), Hefei National Laboratory for Physical Sciences at Microscales, University of Science and Technology of China, Hefei, Anhui 230026, China*

(Received 15 March 2013; revised manuscript received 9 September 2013; published 27 September 2013)

Using scanning tunneling microscopy supplemented with first-principles calculations, we examine all the thermally activated atomistic processes of Ag_n (n = 1–26) constructed atom-by-atom on a Si(111)-(7 × 7) substrate, and we exploit such cluster dynamical information to further determine the energetic stability (or magicity) of the clusters. By generalizing the traditional concept of cluster magicity solely based on cluster association/dissociation to also include various complex collective cluster motions, we identify the existence of two classes of magic clusters. The most stable class, Ag_{10} and Ag_{25}, is defined by geometrical shell closure; the less stable class of Ag_n (n = 3, 5, 13, 16, 19) is associated with lower kinetic barriers against internal restructuring of, or atom detachment from, their respective clusters of neighboring sizes. Our detailed analysis also reveals that the substrate effect, rather than the number of bonds within the clusters, dominates the cluster stabilities. The conceptual advances gained in the present study are broadly applicable to many related cluster systems in contact with external media, and they are expected to be instrumental in tuning the dynamical behaviors of clusters in surface catalysis, nanoplasmonics, and other technological areas.

DOI: 10.1103/PhysRevB.88.125432 PACS number(s): 68.37.Ef, 36.40.Qv, 68.43.Fg, 81.16.Ta

I. INTRODUCTION

Atomic clusters constitute an important class of low-dimensional materials possessing intriguing structures, properties, and functionalities, and many magically sized clusters with exotic physical and chemical properties serve as compelling examples. The traditional definition of cluster magicity relates the cluster stability with the attachment or detachment of a single atom. The extra stabilities relative to their immediate neighboring sizes of the magic clusters are manifested by their higher populations in a typical cluster beam[1–6] or in cluster ensembles fabricated on different substrates.[7–12] Nevertheless, clusters supported on surfaces or in contact with other environments may exhibit qualitatively different dynamical behaviors from their counterparts in free space. For example, clusters on surfaces naturally possess the extra dynamical degrees of collective translation or rotation, which will lead to variations of the cluster-surface contact, thereby causing their stabilities and corresponding magicity to change. Many types of cluster dynamics have been demonstrated recently in real-space observations of various supported clusters.[13–17] It is therefore imperative to generalize the concept of magicity of clusters supported on surfaces (or in other materials settings) by consideration of all the atomic processes, including changes in the surface adsorption site and internal structure, rather than by considerations of single-atom attachment and detachment events alone.

In the field of cluster physics, noble metal clusters on various substrates have been widely studied for their potential applications in nanocatalysis and nanoplasmonics.[18–21] For example, Ag or Au clusters on oxide surfaces were found to exhibit high catalytic activity and selectivity for commercially important reactions such as propylene epoxidation[22,23] and CO oxidation.[24,25] In particular, variations in the clusters' configurations[22] and adsorption sites[24–27] can often influence their catalytic performance, in addition to the demonstrated changes in physical[28–31] or chemical[22,23] properties by adding/removing just one single atom to/from such clusters. The critical role played by the heterogeneous sites is exemplified by Au clusters on TiO_2, with the Ti atoms neighboring Au becoming highly catalytic.[25] These compelling examples convincingly demonstrate that the chemical stabilities of supported clusters critically depend on variations in both the sizes and detailed atomic arrangements of the clusters on the supporting substrates, which are the focus of the present study. The generalized magic clusters, possessing extra stabilities against any type of cluster dynamical processes, are expected to be more durable in various technological applications.

In this paper, we use the prototypical model systems of Ag_n (n = 1–26) clusters formed on Si(111)-(7 × 7) through vertical atomic manipulation with single-atom precision to systematically exploit and validate the concept of generalized cluster magicity. Within this new concept, the magicity of the supported clusters is defined collectively by consideration of all the dynamical processes of the clusters, including collective diffusion, internal restructuring, and association/dissociation. By examining the detailed dynamical movements of the clusters and their magicity, we can convincingly unveil the atomic shell closure and substrate effects as the dominant physical mechanisms working corroboratively in defining the overall stabilities of the supported clusters. The insights gained from the present study are expected to be applicable to many other cluster/substrate combinations as well.[18,19,32,33]

The rest of this paper is structured as follows. In Sec. II, we present our experiment details, including the sample preparation, assembly of Ag clusters, and cluster dynamics measurements. Also, we brief our theoretical calculation methods. In Sec. III, we present our experimental observation of four different types of cluster dynamics of the assembled Ag clusters. We quantitatively measure the rates of their dynamical

processes, from which we define a measure of their stabilities and magicity. Ag clusters with sizes of 10 and 25 are found to be major magic clusters, while sizes of 3, 5, 13, 16, and 19 are found to be minor magic numbers. With theoretical calculations, we determine the atomic structures of Ag_7, Ag_{10}, and Ag_{25} and conclude that the major magic numbers of Ag_{10} and Ag_{25} originate from their geometrical shell closure, whereas the nonmagic number of Ag_7 results from its poor registry with the substrate. We also discuss the correlation between minor magic numbers and the changes in the cluster movement modes. Last, we illustrate that the cluster stabilities within our new definition of magicity are intimately connected with the respective energy differences between their ground states and their corresponding first excited states. We conclude our paper in Sec. V. We also provide two movies showing the dynamical processes of Ag_{16} and Ag_{17} in the Supplemental Material.[34]

II. EXPERIMENT AND THEORETICAL CALCULATION

To quantitatively explore the generalized magicity of supported clusters, we use scanning tunneling microscopy (STM) to reliably determine the cluster sizes and differentiate between the various types of intracluster dynamics. Our experiments are carried out in ultrahigh vacuum with an Omicron variable-temperature STM. An *n*-type Si(111) wafer with a room-temperature resistivity of ∼0.026 Ω cm is used as the substrate. It is cleaned and prepared using standard annealing procedures to form a well-reconstructed Si(111)-(7×7) surface. Ag clusters on Si(111)-(7×7) represent a class of prototypical systems, and the half unit cells (HUCs) of the reconstructed surface naturally act as ideal templates to form identical clusters.[7,9] Ag clusters could be formed by thermal growth with coverages larger than 0.05 monolayer (ML) ($1\ \text{ML} = 1.38 \times 10^{15}\ \text{atoms/cm}^2$).[35] However, this method could neither tell the exact number of atoms of the clusters due to limited resolution of STM images nor provide clean environments for them because of the dense Ag structures on the surface. To precisely identify and quantitatively measure the dynamic processes of the clusters as a function of their sizes, we refer to atomic manipulation to provide such accuracy and clean environments for each cluster.

In our experiment, we deposit ∼0.003 ML Ag onto the Si(111)-(7×7) surface to form single Ag atoms confined in separated HUCs, serving as raw materials for assembling Ag clusters by atomic manipulation.[36] The Ag clusters are prepared by STM vertical atomic manipulation. We take a faulted-HUC (FHUC) of the (7×7) reconstruction as a template trap[35] and use a functionalized STM tip to repetitively transfer single Ag atoms elsewhere to this target FHUC to construct the Ag clusters, one Ag atom at a time. Consequently, the sizes of the clusters can be obtained by counting the number of the Ag atoms used in the assembly.[36] At room temperature, multiple Ag clusters with the same size as well as with different sizes are fabricated in a local area of the surface for subsequent statistical measurements. Sufficient time is allowed at room temperature for the atoms to relax to their equilibrium positions before the clusters are cooled or heated *in situ*. Their dynamical behaviors of the clusters are examined by STM images from low to high temperatures within the range of 95 K to 365 K, to identify their various dynamical movements and to measure the corresponding rates. For changing temperatures, the sample is cooled or heated at a sufficiently low rate to ensure the STM imaging is able to track the same surface area with the prepared clusters.

The STM images are taken at a sample bias of +2 V, together with a small tunneling current of 3 pA to minimize the influence of the STM tip to the atoms, clusters, and their dynamics. All the clusters exhibit certain degrees of rectification behavior,[31] and, as a consequence, an onset sample bias needs to be applied, above which reasonable current responses can be obtained. For clusters from Ag_3 to Ag_{26}, the onset sample bias ranges from +1 V to +2 V. To ensure that all the clusters studied would appear as protrusions, the STM images are taken at a sample bias of +2 V. The influence of the STM tip to the cluster dynamical movements is also examined by varying the sample bias and the tunneling current applied in the measurements, and we conclude that using a sample bias of 2 V and a tunneling current smaller than 100 pA will only bring negligible influence to the movement rate of the clusters.

The structures of a few selected clusters are also simulated within the framework of density-functional theory (DFT) for supercells of about 350 atoms using the VASP code (see Ref. 31 for details).[37]

III. RESULTS AND DISCUSSION

Various types of dynamical processes may destroy the stability of the supported clusters. Although it is impossible to precisely identify the atomic behaviors in each cluster movement, the STM movies could clearly distinguish four qualitatively different movement modes of the clusters, as shown in Fig. 1: (a) "Collective move": A cluster changes its image as an entirety, usually to a symmetrically connected position within the FHUC. This dynamical movement could

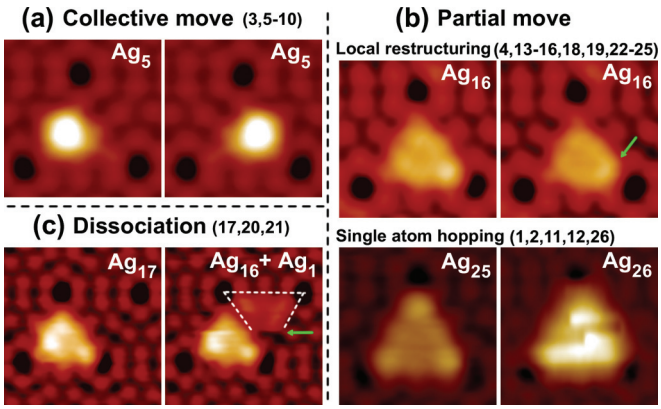

FIG. 1. (Color online) STM images showing four typical modes of movement of the Ag_n (n = 1–26) clusters. (a) Ag_5 moves to a symmetrically connected position as a whole; [(b) upper] Ag_{16} changes its local structure at one corner (marked by the arrow); [(b) lower] Ag_{26} (right) has one single Ag atom diffusing on top of the otherwise static Ag_{25} (left); (c) Ag_{17} dissociates into Ag_{16} and Ag_1, with the dissociation occurring at the line indicated by the arrow. The rest of the clusters can all be classified into one of the movement modes, as listed in the figure.

be understood by collective diffusion of the cluster, either via rotation or translation. An example is Ag_5, which changes its image to its mirror symmetry position, most probably by simultaneously rearranging all or most of the Ag atoms within the cluster. (b) "Partial move": This mode could proceed with a small fraction of a cluster undergoing a collective diffusion while the rest of the cluster stays intact. It includes (i) "local restructuring," which involves a slight image change induced most likely by a rearrangement of the local structure of a given cluster, and (ii) "single-atom hopping," which is caused by one or two fast-moving Ag atoms on top or at the edge of an otherwise static structure. Ag_{16} belongs to the former, for which only a small part of the cluster changes its appearance (indicated by the arrow). Ag_{26} is an example of the latter, for which a single Ag atom diffuses fast on top of the otherwise static Ag_{25} cluster. (c) "Dissociation": A cluster loses one Ag atom to its neighboring HUC and shrinks in size. This process involves detachment of the atom from the cluster and further overcoming the kinetic barrier to leave the original HUC. An example is shown for Ag_{17}, which dissociates into Ag_{16} and Ag_1 in the neighboring HUC, taking place suddenly at the moment labeled by the line change in the image. All the observed cluster dynamics are reversible and represent thermally activated processes between the ground state and metastable configurations. However, we have occasionally observed cluster configuration changes to otherwise unknown structures in some of the long-time measurements. Such changes are irreversible, and they are likely to be caused by the undesirable adsorption processes of the residual gas molecules in the vacuum. In all our data analysis, we have explicitly excluded such spurious events and focused only on the reversible dynamical processes. We have also uploaded movies depicting the "local restructuring" of Ag_{16} and "dissociation" of Ag_{17} in the Supplemental Material.[34] The rest of the clusters in the range Ag_1–Ag_{26} would undergo one of these dynamical movements in our repeated observations.

To investigate the stability of a given cluster, we measure the rate of cluster movement of the first thermally activated mode described above. For each data point at a given temperature, at least 10 events, and most often far more, statistical events are recorded, and the rate averaged. Figure 2(a) shows the rate of movement against temperature, obtained by the exponential fitting of curves $R = a \cdot \exp(-b/T)$ to the measured data points, for clusters Ag_1 to Ag_{26}. Some representative sets of data points are depicted to demonstrate the fitting quality, while the rest of the data points are hidden for better visual clarity. The temperatures facilitating the movement rate of 1–100 times/hour span a large range, but they can be roughly divided into two groups: Those above 200 K are clusters with "collective move," "local restructuring," or "dissociation," and those below 150 K are clusters with "single-atom hopping" (Fig. 1). For the latter, their hopping rates are usually quite fast even at low temperatures (∼100 K). Therefore, the values around 10 times/hour are mostly extrapolated from fittings of much higher measured rates of movement.

We define a stable temperature at which the rate of movement reaches 10 times per hour in order to compare the detailed relative stability among all the clusters. This low movement rate would allow us to observe any intermediate configurations

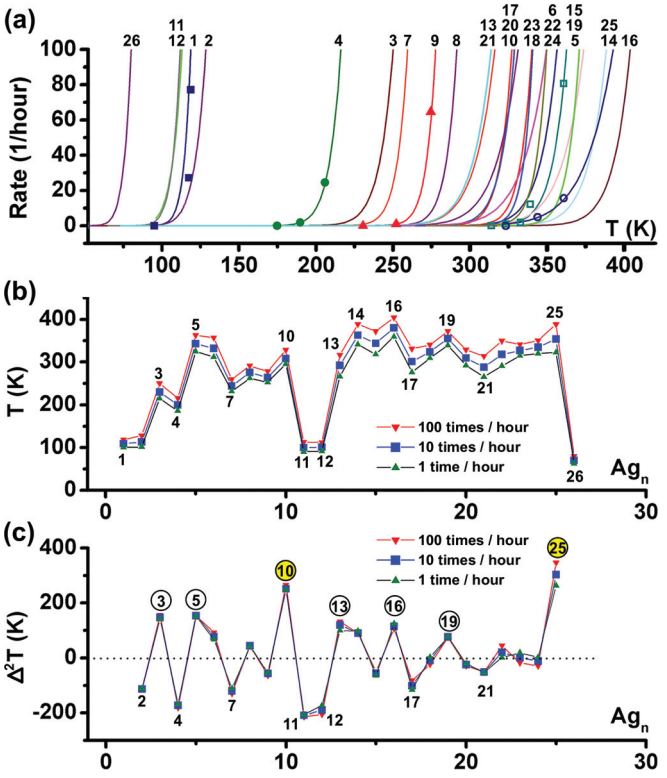

FIG. 2. (Color online) Stabilities of Ag_1–Ag_{26} clusters. (a) The rate of movement for the first thermally activated mode for Ag_1–Ag_{26} at various temperatures. Clusters with nearly bundled curves are labeled by vertically listed numbers, with the topmost number corresponding to the curve attaining the highest temperature at the rate of 100 times/hour. (b) The deduced stable temperature for Ag_1–Ag_{26} defined at three different cluster movement rates. (c) Second-order differences of the stable temperature curves in (b), manifesting the cluster magicities. The two classes of magic clusters are marked by circles of different colors.

if they exist for enough time. The size-dependent stable temperatures for clusters Ag_1 to Ag_{26} can then be extracted from Fig. 2(a), as shown by the curve "10 times/hour" in Fig. 2(b). The stable temperature changes quite substantially for a few neighboring cluster pairs, especially for Ag_2 to Ag_3, Ag_4 to Ag_5, Ag_{10} to Ag_{11}, Ag_{12} to Ag_{13}, and Ag_{25} to Ag_{26}. Using the second-order differences of the stable temperature curve in Fig. 2(b), we obtain the corresponding "10 times/hour" curve in Fig. 2(c), which can better reveal the generalized magicity of the clusters: the major magic numbers of 10 and 25, and the minor magic numbers of 3, 5, 13, 16, and 19. Here, it is important to note that a specific choice for the definition of stable temperature using different rates of movement ranging between 1 and 100 times/hour will only introduce an insignificant shift in the stable temperature curve, as depicted in Fig. 2(b). The stability features as shown in Fig. 2(c), which in essence defines the magicity of the various clusters, strikingly exhibit negligible changes as we vary the rate in the definition. These observations collectively attest to the robust nature of the main findings.

The magicity of Ag_{10} and Ag_{25} arises from the geometrical shell closure of the two clusters. Among all the Ag clusters considered, Ag_{10} and Ag_{25} are the only two that show

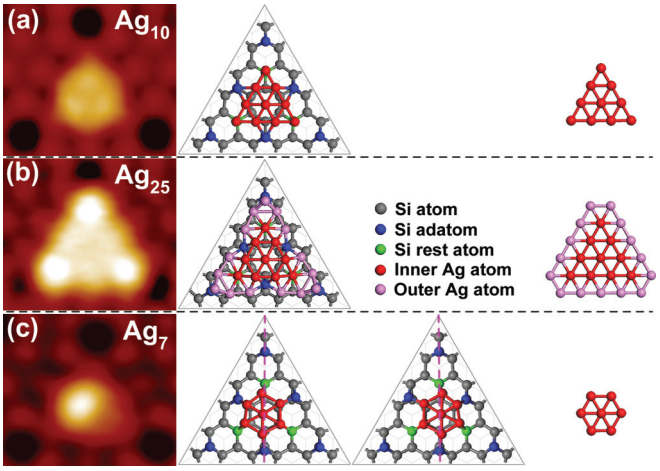

FIG. 3. (Color online) STM images (first column) and DFT structural models (second and third columns) of (a) Ag_{10}, (b) Ag_{25}, and (c) Ag_7 within a FHUC on Si(111)-(7 × 7). The two atomic models for Ag_7 in columns 2 and 3 with different orientations have equivalent structures connected by a mirror symmetry. The last column shows the corresponding free 2D models.

3-fold symmetry in the STM images (Fig. 3), in registry with the substrate symmetry. To correlate the magicity with the geometrical structure of the clusters, we have performed DFT calculations for Ag_{10}, Ag_{25}, and Ag_7, respectively, in a FHUC of Si(111)-(7 × 7) by considering all the Si-Si, Si-Ag, and Ag-Ag interactions in the supercell. The optimized atomic models are shown in Fig. 3. The Ag_{10} structure in Fig. 3(a) shows a good match between the close-packed cluster and the underlying substrate, and thus shows extra stability against Ag_9, primarily due to the loss of freedom to transform among equivalent structures with different orientations. The "single-atom hopping" mode for Ag_{11} and Ag_{12} in Fig. 1 shows that the extra Ag atoms cannot find stable adsorption sites to attach to Ag_{10}. From the evidence of the STM images, the diffusing Ag atoms mostly go along the edge of Ag_{10}, implying that Ag_{10} has no "active" site left to stabilize the extra one or two Ag atoms in Ag_{11} or Ag_{12}. The outer-shell Ag atoms seem to stabilize themselves from Ag_{13} onward. The atomic structure of Ag_{10} persists not only for Ag_{11} and Ag_{12}, but for Ag_{25} (see below), and most likely for all the clusters between Ag_{10} and Ag_{25}. The stable core of Ag_{10} will prevent larger clusters from moving as a whole, as seen in Fig. 1, where no cluster larger than Ag_{10} exhibits "collective move," in contrast to the majority of clusters smaller than Ag_{10}, which can execute such collective moves. The Ag_{25} structure in Fig. 3(b) shows a similar shell closure to Ag_{10}, with a similar inner Ag_{10} structure (red), and additional 15 Ag atoms (purple) filling the outer sites to form another complete shell. The STM image of Fig. 1 indicates that the extra Ag atom in Ag_{26} cannot find a binding site at the edge of Ag_{25} for attachment and can only diffuse fast on top of Ag_{25}.

The substrate can play an important role in stabilizing the supported clusters and defining their corresponding magicity. In a free two-dimensional (2D) cluster model, as shown in the right column of Fig. 3, Ag_7 would also have 3-fold symmetry and be more stable than Ag_{10} because every Ag atom would at least form three bonds with the neighbors. However, neither the STM imaging nor the stability analysis reveals any extra magicity of Ag_7. In the DFT optimized atomic model in Fig. 3(c), though Ag_7 forms a nearly 3-fold symmetric structure, it does not overlay symmetrically with the substrate. Rather, it leans to one side of the FHUC. The mismatch between Ag_7 and the underlying Si(111)-(7 × 7) is expected to result in a reduced stability, as shown in Fig. 2(b), as the Ag atoms in Ag_7 will need to move only a small distance to transform into its equivalent structure, as shown in Fig. 3(c). With each of the three corner Ag atoms only forming two bonds with its neighboring Ag atoms, the extra stability of Ag_{10} could originate from the bond between the corner Ag atom and the underneath Si rest atom. Unlike the free 2D structure of Ag_{25} in Fig. 3(b), the DFT simulated atomic structure of Ag_{25} does not show a close-packed arrangement. Here, by replacing three Ag atoms with center Si-adatoms and moving the respective Ag atoms to the corners to bind with the corner Si adatoms, the resulting structure gains its extra stability. These observations demonstrate that, because of the possibility to bind with the surface Si atoms, the supported Ag clusters cannot be considered as free 2D clusters, and their magicity is at variance with the expectations from the planner atomic model via a simple bond counting analysis of the Ag atoms.

Similar to the major magic clusters of Ag_{10} and Ag_{25}, the minor magic numbers also correlate well with the changes in the movement modes. As seen from the list in Fig. 1, Ag_3 and Ag_5 gain their metastabilities because the dynamics of these two clusters is via "collective move," while their common neighbor of Ag_4 possesses lower stability via "local restructuring." Similarly, Ag_{13} gains its metastability because its primary mode of dynamics is "local restructuring," which is more difficult than the low-kinetic-barrier "single-adatom-hopping" mode of its neighboring cluster of Ag_{12}. Ag_{16} and Ag_{19} gain their metastabilities because their primary mode of dynamics is also "local restructuring," which is also more difficult than the primary "dissociation" mode of their respective neighbors of Ag_{17} and Ag_{20}.

The above points can be further illustrated pictorially. Because the observed cluster dynamics refers to the first thermally activated mode of a given cluster, the generalized magicity can be understood from the respective energy levels. Figure 4(a) shows a schematic drawing of the relative energy

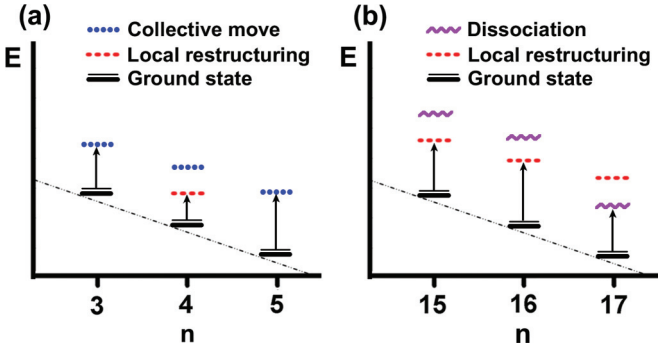

FIG. 4. (Color online) The plausible energy levels for various movement modes for Ag_3–Ag_5 (a) and Ag_{15}–Ag_{17} (b), respectively. The dashed oblique line represents a binding energy increase with the cluster size. All the energy values are plotted only for qualitative comparison.

levels of Ag_3, Ag_4, and Ag_5. The three clusters can all undergo a "collective move" to transform to their equivalent structures, similar to Ag_5 shown in Fig. 1. The required excitation temperatures are found to increase with the cluster sizes, since more and more atoms are involved in this movement mode. This is represented by gradually increased energy separation between the "collective move" state and the "ground state." Nevertheless, while the "collective move" is the first excitation for Ag_3 and Ag_5, Ag_4 can be excited first to another metastable state via "local restructuring," which has a lower barrier, involves fewer numbers of atoms, and occurs at much lower temperature (∼200 K vs 333 K). Figure 4(b) shows a possible energy diagram of Ag_{15}, Ag_{16}, and Ag_{17}. The states of "dissociation" represent the energy barrier for the clusters to dissociate. Though the "dissociation" states of Ag_{15} and Ag_{16} or the "local restructuring" state of Ag_{17} are not observed in the experiments, they are considered as the higher excited states. The first excitation energy for Ag_{17} is relatively smaller than those of Ag_{15} and Ag_{16}, as seen from the data points in Fig. 1(b), and it makes "dissociation" as its first excitation mode to contribute to the stability of Ag_{16} by contrast.

IV. CONCLUSION

In conclusion, we have used a set of Ag clusters on Si(111) as the prototypical systems to effectively establish the new concept of generalized magicity of nanoclusters in close contact with environmental settings. To our best knowledge, this is the first attempt to go beyond the traditional definition of cluster magicity defined by consideration of single-atom attachment or detachment alone, as well as the first experimental exploration of the dynamical processes of supported clusters as a function of the cluster size with single-atom precision. By examining the various cluster dynamical processes in terms of collective diffusion, internal restructuring, and the traditional single-atom attachment/detachment for the Ag_1–Ag_{26} clusters, we clearly demonstrate the existence of two classes of magic clusters, with the most stable class consisting of Ag_{10} and Ag_{25} and the less stable class consisting of Ag_3, Ag_5, Ag_{13}, Ag_{16}, and Ag_{19}. The magic sizes are found to be well correlated with the geometrical structures of the respective clusters and are strongly influenced by the substrate. From an energetic perspective, the stabilities of the clusters are intimately connected with the respective energy differences between their ground states and their corresponding first excited states. This new concept of generalized magicity embodies rich physical contents, and it is expected to play a vital role in future rationalization of various dynamical phenomena and related stabilities of a vast variety of supported nanoclusters with desirable functionalities.

ACKNOWLEDGMENTS

This work was supported by the Direct Grant for Research (Grant No. 4053017) from the Chinese University of Hong Kong and the Research Grants Council of Hong Kong (Grant No. 403311). Z.Y.Z. acknowledges support by National Natural Science Foundation of China (Grant No. 11034006).

*Corresponding authors: zhangzy@ustc.edu.cn; xdxiao@phy.cuhk.edu.hk

[1] W. D. Knight, K. Clemenger, W. A. de Heer, W. A. Saunders, M. Y. Chou, and M. L. Cohen, Phys. Rev. Lett. **52**, 2141 (1984).
[2] H. W. Kroto, J. R. Heath, S. C. O'Brien, R. F. Curl, and R. E. Smalley, Nature (London) **318**, 162 (1985).
[3] J. Li, X. Li, H. J. Zhai, and L. S. Wang, Science **299**, 864 (2003).
[4] H. Haberland, T. Hippler, J. Donges, O. Kostko, M. Schmidt, and B. von Issendorff, Phys. Rev. Lett. **94**, 035701 (2005).
[5] N. Shao, W. Huang, Y. Gao, L.-M. Wang, X. Li, L.-S. Wang, and X.-C. Zeng, J. Am. Chem. Soc. **132**, 6596 (2010).
[6] P. Jena, J. Phys. Chem. Lett. **4**, 1432 (2013).
[7] J. L. Li, J. F. Jia, X. J. Liang, X. Liu, J. Z. Wang, Q. K. Xue, Z. Q. Li, J. S. Tse, Z. Y. Zhang, and S. B. Zhang, Phys. Rev. Lett. **88**, 066101 (2002).
[8] H. G. Boyen, G. Kästle, F. Weigl, B. Koslowski, C. Dietrich, P. Ziemann, J. P. Spatz, S. Riethmüller, C. Hartmann, M. Möller, G. Schmid, M. G. Garnier, and P. Oelhafen, Science **297**, 1533 (2002).
[9] H. H. Chang, M. Y. Lai, J. H. Wei, C. M. Wei, and Y. L. Wang, Phys. Rev. Lett. **92**, 066103 (2004).
[10] Y.-P. Chiu, L.-W. Huang, C.-M. Wei, C.-S. Chang, and T.-T. Tsong, Phys. Rev. Lett. **97**, 165504 (2006).
[11] R. Zhou, X.-H. Wei, K. He, J. E. Shield, D. J. Sellmyer, and X.-C. Zeng, ACS Nano **5**, 9966 (2011).
[12] S. V. Ong and S. N. Khanna, J. Phys. Chem. C **116**, 3105 (2012).
[13] F. Silly and M. R. Castell, ACS Nano **3**, 901 (2009).
[14] Z. W. Wang and R. E. Palmer, Nano Lett. **12**, 5510 (2012).
[15] M. T. McDowell, I. Ryu, S. W. Lee, C.-M. Wang, W. D. Nix, and Y. Cui, Adv. Mater. **24**, 6034 (2012).
[16] S. I. Sanchez, M. W. Small, E. S. Bozin, J.-G. Wen, J.-M. Zuo, and R. G. Nuzzo, ACS Nano **7**, 1542 (2013).
[17] D. Shao, X. Liu, N. Lu, C.-Z. Wang, K. M. Ho, M. C. Tringides, and P. A. Thiel, Surf. Sci. **606**, 1871 (2012).
[18] K.-H. Meiwes-Broer (ed.), *Metal Clusters at Surfaces, Structure, Quantum Properties, Physical Chemistry* (Springer-Verlag, New York, 2000).
[19] D. Mulugeta, K. H. Kim, K. Watanabe, D. Menzel, and H.-J. Freund, Phys. Rev. Lett. **101**, 146103 (2008).
[20] M. Rycenga, C. M. Cobley, J. Zeng, W.-Y. Li, C. H. Moran, Q. Zhang, D. Qin, and Y.-N. Xia, Chem. Rev. **111**, 3669 (2011).
[21] N. J. Halas, S. Lal, W. S. Chang, S. Link, and P. Nordlander, Chem. Rev. **111**, 3913 (2011).
[22] Y. Lei, F. Mehmood, S. Lee, J. Greeley, B. Lee, S. Seifert, R. E. Winans, J. W. Elam, R. J. Meyer, P. C. Redfern, D. Teschner, R. Schlögl, M. J. Pellin, L. A. Curtiss, and S. Vajda, Science **328**, 224 (2010).
[23] W. E. Kaden, T. Wu, W. A. Kunkel, and S. L. Anderson, Science **326**, 826 (2009).

[24]M. S. Chen and D. W. Goodman, Science **306**, 252 (2004).
[25]I. X. Green, W. Tang, M. Neurock, and J. T. Yates, Jr., Science **333**, 736 (2011).
[26]P. L. Hansen, J. B. Wagner, S. Helveg, J. R. Rostrup-Nielsen, B. S. Clausen, and H. Topsøe, Science **295**, 2053 (2002).
[27]M. Stamatakis, M. A. Christiansen, D. G. Vlachos, and G. Mpourmpakis, Nano Lett. **12**, 3621 (2012).
[28]R. Moro, X. Xu, S. Yin, and W. A. de Heer, Science **300**, 1265 (2003).
[29]K. Joshi, S. Krishnamurty, and D. G. Kanhere, Phys. Rev. Lett. **96**, 135703 (2006).
[30]G. A. Breaux, D. A. Hillman, C. M. Neal, R. C. Benirschke, and M. F. Jarrold, J. Am. Chem. Soc. **126**, 8628 (2004).
[31]S. Hu, A. Zhao, E. Kan, X. Cui, X. Zhang, F. Ming, Q. Fu, H. Xiang, J. Yang, and X. Xiao, Phys. Rev. B **81**, 115458 (2010).
[32]C. Binns, Surf. Sci. Rep. **44**, 1 (2001).
[33]A. T. N'Diaye, T. Gerber, C. Busse, J. Mysliveček, J. Coraux, and T. Michely, New J. Phys. **11**, 103045 (2009).
[34]See Supplemental Material at http://link.aps.org/supplemental/10.1103/PhysRevB.88.125432 for two movies showing the dynamic processes of Ag_{16} and Ag_{17}.
[35]F. Ming, K. Wang, X. Zhang, J. Liu, A. Zhao, J. Yang, and X. Xiao, J. Phys. Chem. C **115**, 3847 (2011).
[36]F. Ming, K. Wang, S. Pan, J. Liu, X. Zhang, J. Yang, and X. Xiao, ACS Nano **5**, 7608 (2011).
[37]G. Kresse and J. Furthmüller, Phys. Rev. B **54**, 11169 (1996).